Impact of gold-mining activity on trace elements enrichment in the West African estuaries: The case of Pra and Ankobra rivers with the Volta estuary (Ghana) as the reference

Emmanuel Klubi, José M. Abril',*, Elvis Nyarko',[1], Antonio Delgado

A B S T R A C T

This study aimed at assessing trace element concentrations in two representative estuaries of Ghana (Pra and Ankobra) affected by gold-mining, relative to the levels of the unaffected Volta estuary. Surficial sediments (n = 16–17) were sampled at each estuary and analysed by ICP-MS for 25 elements after pseudo-total digestion. The enrichment and geoaccumulation indexes revealed a moderate to significant contamination of As, Ag and Cu in the Pra and Ankobra estuaries. Spatial maps of concentrations revealed non-localized sources. High As con-centrations were attributable to runoff transport and sedimentation of gold mining-tailing particles, as suggested by results from granulometric distributions, correlation and PCA analysis. The probabilities of surpassing the probable effects level (PEL) were 77% for As, 50% for Cr and 27% for Ni in Ankobra; these values were of 13%, 23% and 10% for the Pra. Results reveal potential future implications on ecosystems and human health in these both estuaries as result of the gold-mining activity.

Keywords:
Volta Estuary
Pra Estuary
Ankobra Estuary
Gold mining
Trace-elements
ICP-MS analysis

1. Introduction

Estuaries are effective sediment traps due to their particular hydrodynamics and to the salinity induced sediment flocculation (Postma, 1967; Allen et al., 1980). Contamination of estuarine sediments is of broad concern since they represent one of the ultimate sinks for pollutants discharged into the aquatic environment. They reflect the proximity of the contamination sources and can preserve the fingerprint of the range of chemical, oceanographic, geological and anthropogenic factors, which govern the distribution of trace elements (Bryan and Langston, 1996; Olmos and Birch, 2008; Magesh et al., 2011; Mil-Homens et al., 2014; Xu et al., 2014). This makes these aquatic environments of particular interest for assessing anthropogenic impacts (Pan and Wang, 2012).

Among estuaries, those affected by mining activities are of special concern since they can be severely polluted aquatic environments (López-González et al., 2006; Doe et al., 2017). One of the major impacts comes from the artisanal and small-scale gold mining, where the use of mercury (Hg) for amalgamation is common, with associated yearly discharges to the environment of this metal of 650–1000 tons (Adjei-Kyereme et al., 2015). In West Africa, Ghana is the most representative case of this exploitation of natural resources, with half of the total gold production in the region (World Bank, 2012; Chuhan-Pole et al., 2017).

In May 1989, the use of Hg in small-scale gold mining was legalized in Ghana (Provisional National Defence Council Law 218). This has increased these mining activities, which nowadays provides employment to over one million people (Donkor et al., 2006). The greater part of gold production (about 81%) in Ghana comes from goldfields in its southwestern region (Fig.1), an area of about 40,000 km^2 which is drained by three main rivers: Tano, Ankobra, and Pra (Donkor et al., 2006).

To separate the gold (Au), Hg is mixed with the mineral bearing rock to form an amalgam. The burning of the amalgam leads to vaporization and spreading of Hg into a toxic plume (Pfeiffer and Lacerda, 1988). Mercury also reaches the streams of water, where it poses a great threat for the environment and human health (Oduro et al., 2012). A brief review on health effects due to exposures to Hg can be seen at the US-EPA website (www.epa.gov/mercury). Although much attention has been paid to gold-mining related Hg pollution, this is not the only concern derived from this activity.

Tailings are a mixture of finely ground rock resulting from the

* Corresponding author at: Departamento de Física Aplicada I, ETSIA, Universidad de Sevilla, Carretera de Utrera km 1, D.P. 41013 Sevilla, Spain.
E-mail address: jmabril@us.es (J.M. Abril).
[1] Prof. Elvis Nyarko is also the Vice Chancellor of the Regional Maritime University, Accra, Ghana.

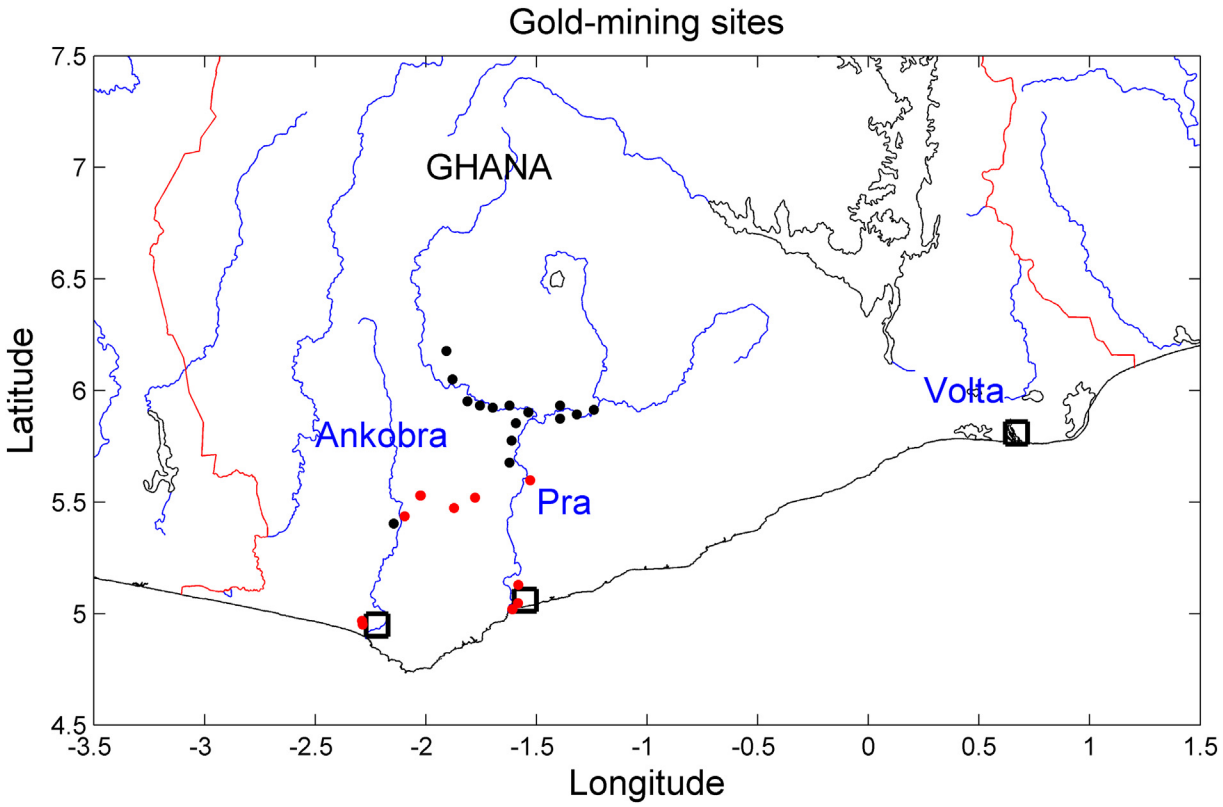

Fig. 1. Map of Ghana with the course of the rivers Ankobra, Pra and Volta. Black dots are gold-mining sites reported by Donkor et al. (2005) along the Pra, and the site of Tarkwa, next to Ankobra. Red dots are gold-mining sites identified for this work in a survey with local communities. There are not official logs, and the above identified sites represent only a fraction of the small-scale gold mines covering the entire Ankobra and Pra basins. Artisanal gold-miners move almost daily from spot to spot to dig out for gold. Rectangles delimit the three estuarine areas studied in this work. (For interpretation of the references to color in this figure legend, the reader is referred to the web version of this article.)

retrieval of gold and water used in the processing. They may contain significant concentrations of potentially toxic elements. Arsenic (As) in mine tailings usually exists as sulfide minerals such as arsenopyrite [FeAsS], realgar [As_2S_2] and orpiment [As_2S_3]. Zinc (Zn) and lead (Pb) occur in gold ore bodies in the form of sphalerite [ZnS] and galena [PbS], respectively, while copper (Cu) appears in sulphides, arsenites, chlorides and carbonates, and chromium (Cr) in chromates [$FeCr_2O_4$] (Fashola et al., 2016).

In the mining tailings exposed to the air, oxidation of sulfide minerals results in the release of As and other potentially toxic elements, thus promoting the contamination of the surrounding soil and waters (Lim et al., 2009). Tailings spillages are more drastic pathways of pollution which can occur by flood damages and ground subsidence (Bempah et al., 2013).

Environmental risk assessment of the sediment compartment is a complex task which is subject to intense debate (Tarazona et al., 2014). It is necessary a proper problem definition (hazardous elements, target organisms, and level of protection required) and a conceptual model for exposure and effect assessments. This requires a detailed knowledge on the sedimentological and biotic characteristics and on the dynamics of the studied system. Sediment quality guidelines (SQGs), based upon the definition of reference toxicity values, can be used for screening purposes.

A series of reference concentrations in sediments have been defined for a wide set of elements (Macdonald et al., 1996), such as the lower 10th-percentile concentration associated with observation of biological effects (effect range low, ERL) and the probable effects level (PEL). These screening levels are widely used in the scientific literature to assess the consequences of pollution (e.g., Suresh et al., 2012; Pereira et al., 2015; Ennouri et al., 2016). Other pollution indexes are based on the comparison with suitable reference levels (Loring and Rantala, 1992).

Current data available in West Africa are mostly focused on Hg and As (Amonoo-Niezer et al., 1996; Bannerman et al., 2003; Donkor et al., 2006; Asante and Ntow, 2009; Rajaee et al., 2015; Adjei-Kyereme et al., 2015). Donkor et al. (2005) measured Hg, Al, Fe, As, Pb, Cu, Cr, Ni, Mn, Co, V, and Zn in sediments sampled along the course of the Pra River. In spite of above referred studies, there is a lack of knowledge on how the gold mining activities in West Africa may increase the concentrations of a wide set of harmful trace-elements in waterbodies and estuarine environments.

The aim of this study was the assessment of major and trace-metal concentrations in surface sediments from three representative estuarine environments in Ghana, in order to explore their natural and anthropogenic inputs. The target elements were Be, B, Al, Ti, V, Cr, Mn, Fe, Co, Ni, Cu, Zn, As, Se, Sr, Mo, Ag, Cd, Sb, Cs, Ba, Tl, Pb, Th, U and Hg. In the absence of site-specific sediment quality guidelines, this work adopts reference values and SQGs from scientific literature as a preliminary and logical step. The core of the proposed methodology is however the comparison at regional scale of sediments from estuaries potentially affected (Pra and Ankobra) with other free of gold mining activities (the Volta estuary).

2. Materials and methods

2.1. The studied estuaries

This study was conducted in three major estuaries (Volta, Pra and Ankobra) in the coastal belt of Ghana (see Fig. 1). There are no official logs on gold-mining sites in Ghana. Fig. 1 shows some of them in the

Fig. 2. Satellite images (from Google Earth) of the Volta, Pra and Ankobra estuaries in Ghana. The locations of the sampling sites of surficial sediments used in this study are depicted. For the Ankobra estuary, the sampling points used for the granulometric analyses (AS1 to AS4) are also depicted.

Pra and Ankobra basins, based on data by Donkor et al. (2005) and on a survey conducted with local communities for this study. In this rural south-western portion of Ghana the lack of industrial activities makes small-scale gold mining the main source of water resource contamination with potentially toxic elements (Donkor et al., 2005).

Two types of gold-bearing ores are mined in Ghana: i) quartz vein (quartz with free gold in association with lesser amounts of various metals) and ii) sulphide ores (arsenopyrite), associated with gold, iron, zinc, lead and copper (Nude et al., 2011). A more detailed study on the mineralogy of the gold deposits in Ghana can be seen in Milési et al. (1991). Studies on gold mining tailings are scarce. Bempah et al. (2013) studied active and abandoned tailing dams at Obuasi, Ghana. The texture of tailings was of silty clay loam to clay. They reported concentrations ranging from 542 to 1752 $mg{\cdot}kg^{-1}$ for As, from 129 to 1848 $mg{\cdot}kg^{-1}$ for Mn, from 24 to 92 $mg{\cdot}kg^{-1}$ for Cu, from 79.5 to 204 $mg{\cdot}kg^{-1}$ for Zn and from 4.1 to 75% for Fe.

The Pra and Ankobra estuaries are located in the Ghana's Western Region, a tropical rain forest zone. Its geology is associated with alluvial gold deposits in basal rock underlying by meta-sedimentary and volcanic of the Birimian and Tarkwaian systems. The Pra estuary is located in the eastern side of the Shama Township. The River Pra originates from the Mampong-Kwahu and Atiwa Ranges with multiple tributaries (Offin, Oda and Birim). The estuary received additional water flow from two adjoining tributes at the east and west respectively. It forms a network of multiple channels lying parallel to the coastline with islands mostly flooded during high tides and in the wet season. Mangrove is the dominant vegetation, which provides suitable habitat for crabs, fish and avifauna at the lower section of the river which is a fishing site.

The Ankobra estuary in Asanta, Nzema East district, is the lower section of River Ankobra which takes its source from the North hills of Basindare, near Bibiani. It is joined in the mid-section by rivers Mansi, Ankasa and Bonsa. The entrance of the estuary could be described as a sand ramp with abrupt increase in depth towards the freshwater end. The water column is extremely turbid. The riparian vegetation, mainly mangrove, provides niches for avifauna. The immediate west coastline comprises beaches with coconut plants providing defences structure for sand dunes. The estuary also serves as fish landing site for the local community.

The Volta estuary in Ada-Foah is located in the Dangbe East District of the Greater-Accra Region about 90 km from Accra. The river Volta watershed extends on Niger, Cote d'Ivoire, Burkina Faso and Togo, it being the largest river in West Africa. This river drains about 70% of the Ghana's hydrological basin and has two hydro-dams built on it in 1965 and 1982. Its estuary forms a delta system flagged on its east and west by the Keta lagoon complex and the Songhor lagoon respectively. Coconut and mangrove dominate the vegetation cover at its peripheries while the bottom floor provides suitable habitat for the *Galatea paradoxa*, as well as other benthic fauna. The estuary also provides transport facilities for the communities and it is a recognized touristic site.

Mahu (2014) reported granulometric and mineralogical characterizations of sediments cores sampled at the above three estuaries. Mean grain sizes ranged from 27.5–37.8 μm, 15.9–41.2 μm and 20.1–64.9 μm in the Ankobra, Pra and Volta estuaries, respectively. Non-biogenic materials constituted about 100% and 96% in the Ankobra and Pra estuaries, while they ranged from 80% to 95% in the Volta estuary. In the three cores quartz made the bulk of non-biogenic materials. According to the geological map of Ghana (see Petersson et al., 2018), the Volta estuary is dominated by alluvial sediments and continental clastic sedimentary rocks, while around the Pra and Ankobra estuaries meta-volcanic rocks are dominant.

Klubi et al. (2017) reported recent ^{210}Pb-based sediment accumulation rates in sediment cores from the Volta and Pra estuaries, being of $1.05 \pm 0.03\ g\ cm^{-2}\ year^{-1}$ and $2.73 \pm 0.06\ g\ cm^{-2}\ year^{-1}$, respectively.

2.2. Sampling, sample preparation and ICP-MS analysis

Surface sediment samples were collected from each of the studied estuaries (n = 16–17), between 27th January and 5th February 2017, covering a representative area (see Fig. 2). Precise positioning of each sampling location was done using a Garmin Extrex GPS. Sampling depths ranged from 1 to 15 m, with the deepest location in the Ankobra estuary. Samples were grabbed using Ekman grab and transferred into pre-labelled Ziplock bags, sealed and placed in a cooler and further stored frozen in the Marine and Fisheries' laboratory in the University of Ghana. The sediment samples were latter thawed, dried at 50 °C using a Gallen Kamp Plus II oven to a constant weight, and re-packaged and transported to the Agricultural Research Service laboratory (SIA-CITIUS) of the University of Seville, Spain.

The largest percentage of the anthropogenic-derived potentially toxic elements in sediments is often found in their most fine particles (Abril and Fraga, 1996; Islam and Tanaka, 2004). In the scientific literature some authors adopt the criterion of analyzing the studied elements only in the grain size fraction under 63 µm (e.g., Ennouri et al., 2016) while others measure the bulk sample considering the grain-size fraction lower than 2 mm (e.g. Wei and Wen, 2012; Dimitrakakis et al., 2014). The second criterion has been adopted in this work.

A large variety of methods have been published for acid digestion of environmental samples for elemental analysis. For those elements with fractions associated with silicates, many studies do digestion with HF, but this requires rigorous safety protocols and the use of H_3BO_3 for redissolving fluoride precipitates (Gerboles et al., 2011), with the operational problems that this entails. Many other studies use digestion procedures based on the US-EPA 3051A methodology for pseudo-total digestion. It is worth noting that this last method applied to soil and sediment samples provides a reasonable estimation of leachable/total contents of elements (Link et al., 1998; Gelinas et al., 1998). Elements determined after this digestion are usually more representative of the available fraction since there is no bias introduced by the variable amount of non-reactive residual material. This US-EPA 3051A method (US-EPA, 1995) has been used in this work also considering the use of H_2O_2 for enhancing organic matter mineralization. The adopted criterion of measuring acid-digested trace-elements in the bulk sediment was also congruent with trend-lines in probabilistic risk assessment studies (Twining et al., 2008).

For microwave-assisted acid digestion, ca. 0.25 g of powdered sediment was mixed with 4.5 mL of nitric acid (69% HNO_3), 1.5 mL of hydrochloric acid (36% HCl) and 0.5 mL of hydrogen peroxide (30% H_2O_2). All reagents were of Suprapur grade (Merck, Darmstadt, Germany). For closed-vessel digestions, a microwave system Milestone Ethos was used. The digests were then diluted with 18 MΩ cm deionized water to a fixed volume of 100 mL, and allowed to settle for 48 h at 4 °C.

After digestion, trace elements were determined at the SIA-CITIUS of the University of Seville using an Inductively Coupled Plasma Mass Spectrometry system ICP-MS X7 (Thermo Fisher, Cambridge, UK) with quadrupole mass analyzer, multichannel detector (Pulse Counting and Analog Methods), auto sampler ASX-500 (CETAC, Omaha, NE, USA) and software Plasma Lab version v2.5.4. Details on the instrumental settings, correction equations, quality controls and sample lists can be found in Enamorado-Báez et al. (2013).

Fully quantitative determinations were done for Be, B, Al, Ti, V, Cr, Mn, Fe, Co, Ni, Cu, Zn, As, Se, Sr, Mo, Ag, Cd, Sb, Cs, Ba, Tl, Pb, Th and U with three main runs. In addition, for each sample a full spectrum was acquired with the instrument in survey mode (10 cannels per mass, with 10 sweeps, and a dwell time of 0.6 ms). Long pre-acquisition and washing times of 90 s each were used to minimize memory effects. The net area of the peak for the *m/z* ratio 202 (Hg) was estimated by subtraction of the nearest reagent blank, and quantified through the count rate found for the certified reference material IAEA-405. This provided a semi-quantitative estimation of the Hg concentration levels in the studied samples. It is worth noting that the total recoverable sample digestion procedure and the above standard settings for ICP-MS measurements are not suitable for fully quantification of Hg (section 1.6, EPA 200.8 method).

2.3. Quality assurance

Methods were tested through the measurement of several analytical replicates of the certified reference materials (CRM) IAEA-405 (estuarine sediment, supplied by the Analytical Quality Control Services from the International Atomic Energy Agency). Different data quality tests were carried out during instrumental running using some recommendations provided by US-EPA 200.8 methodology, such as analytical replicate samples, matrix matching and memory effects, as

Table 1
Method detection limits (MDL) for the studied elements and measurements of the certified material IAEA-405.

Element	*m/z*	MDL	IAEA-405 Estuarine sediment		
			Measured	Certified	Recovery
		mg·kg^{-1}	mg·kg^{-1}		%
Be	9	0.04	2.5 ± 0.2	N.R.	
B	11	0.40	10.1 ± 0.5	N.R.	
Al	27	45	50,000 ± 7000[b]	78,000 ± 5000[a]	64 ± 10
Ti	49	1.7	900 ± 60[b]	N.R.	
V	51	6.5	50 ± 5	95 ± 5	53 ± 7
Cr	52	2.0	56 ± 2	84 ± 4	67 ± 4
Mn	55	0.5	520 ± 50[b]	495 ± 11	104 ± 10
Fe	57	50	37,200 ± 800[b]	37,400 ± 700	99 ± 4
Co	59	0.3	12.9 ± 0.6	13.7 ± 0.7	94 ± 7
Ni	60	0.3	27.9 ± 1.0	32.5 ± 1.4	86 ± 5
Cu	65	0.4	37 ± 2	47.7 ± 1.2	78 ± 4
Zn	66	0.08	208 ± 6	279 ± 14	75 ± 3
As	75	1.6	17.8 ± 0.6	23.6 ± 0.7	84 ± 4
Se	82	1.5	< MDL	0.44 ± 0.12	
Sr	88	0.5	108 ± 11	118 ± 14[a]	92 ± 16
Mo	98	0.11	0.49 ± 0.03	N.R.	
Ag	107	0.013	0.96 ± 0.09	N.R.	
Cd	111	0.014	0.75 ± 0.01	0.73 ± 0.05	103 ± 7
Sb	123	0.10	1.77 ± 0.09	1.8 ± 0.4	98 ± 12
Cs	133	0.2	8.3 ± 0.2	12.5 ± 2.1[a]	66 ± 12
Ba	137	0.6	98 ± 6	N.R.	
Hg	202	N.Q.		0.81 ± 0.04	
Tl	205	0.011	0.60 ± 0.02	N.R.	
Pb	208	0.09	72 ± 3	75 ± 4	96 ± 6
Th	232	0.05	13.8 ± 0.6	14.3 ± 2.1[a]	96 ± 15
U	238	0.007	1.93 ± 0.08	3.0 ± 1.2[a]	64 ± 25

Microwave-assisted acid digestion method (see Methods' section).
Measured values are reported as the mean and standard deviation of the mean (three analytical replicates), while certified values are provided with 95% confidence interval. N.R.: not reported values; N.Q: not quantified. The *m/z* ratio identifies the isotope used for quantification. Details on correction equations for isobaric and polyatomic interferences can be seen in Enamorado-Báez et al. (2013).

[a] Reference values.

[b] Extrapolate from the calibration curve.

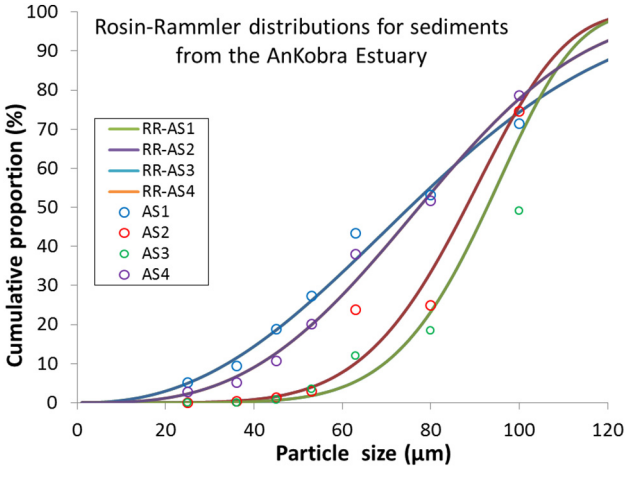

Fig. 3. Results (dots) from the granulometric analysis of samples AS1 to AS4 from the Ankobra estuary (see Fig. 2), given as cumulative proportion vs grain size. Continuous lines are the corresponding fitted Rosin-Rammler distributions.

Table 2
Element concentration (mg·kg^{-1} unless specified otherwise) in the sediment samples (mean and SD) from the Volta (n = 17), Pra (n = 16) and Ankobra (n = 17) estuaries, in Ghana; compared against the ERL and PEL values[†] and the reference levels[‡].

Element	m/z	Volta	Pra	Ankobra	ERL	PEL	Ref. level
Be	9	0.64 ± 0.33 (b)	0.96 ± 0.34 (a)	0.95 ± 0.33 (a)			2.1^{EC}
B	11	5.1 ± 3.3 (a)	3.4 ± 1.6 (b)	3.6 ± 1.2 (b)			17^{EC}
Al[§]	27	4.2 ± 2.8 (b)	8.4 ± 4.0 (a)	8.1 ± 3.4 (a)			11.3^{AR}
Ti	49	370 ± 120 (ab)	400 ± 110 (a)	306 ± 75 (b)			4400^{WR}
V	51	39[*] (c)	94 ± 34 (b)	154 ± 53 (a)			116^{AR}
Cr	52	36 ± 16 (c)	85 ± 32 (b)	123 ± 46 (a)	81t[#]	160	130^{AR}
Mn	55	1800 ± 1500 (a)	245 ± 100 (b)	261 ± 71 (b)			1478^{AR}
Fe[§]	57	2.9 ± 1.3 (b)	4.2 ± 1.1 (a)	4.1 ± 1.3 (a)			7.5^{AR}
Co	59	7.7 ± 4.3 (b)	15.5 ± 3.6 (a)	13.6 ± 3.6 (a)			23^{AR}
Ni	60	12.2 ± 6.6 (b)	23.7 ± 8.1 (a)	25.0 ± 8.2 (a)	21	42.8	78^{AR}
Cu	65	6.4 ± 4.3 (b)	23.1 ± 7.1 (a)	23.8 ± 7.9 (a)	34	108	53^{AR}
Zn	66	21 ± 10 (b)	51 ± 13 (a)	53 ± 15 (a)	150	271	130^{AR}
As	75	5.7 ± 3.0 (c)	23.0 ± 9.2 (b)	50 ± 13 (a)	8.2t[#,&]	41.6	4.8^{EC}
Se	82	< MDL	< MDL	< MDL	1.0	1.77	0.09^{EC}
Sr	88	240 ± 150 (a)	45 ± 22 (c)	120 ± 40 (b)			187^{WR}
Mo	98	0.29 ± 0.26 (b)	0.59 ± 0.33 (a)	0.67 ± 0.19 (a)			2.98^{WR}
Ag	107	0.03 ± 0.02 (b)	0.10 ± 0.03 (a)	0.12 ± 0.02 (a)			0.053^{EC}
Cd	111	0.06 ± 0.12 (b)	0.09 ± 0.02 (a)	0.07 ± 0.02 (a)	1.2	4.21	0.09^{EC}
Sb	123	0.26 ± 0.13 (c)	0.47 ± 0.10 (b)	1.01 ± 0.21 (a)			2.19^{WR}
Cs	133	0.81 ± 0.61(b)	2.64 ± 0.96 (a)	2.47 ± 0.94 (a)			6.25^{WR}
Ba	137	38 ± 33 (b)	80 ± 36 (a)	100 ± 39 (a)			402^{AR}
Hg[‖]	202	0.075 ± 0.057 (c)	0.20 ± 0.17 (b)	0.28 ± 0.10 (a)	0.15t[¶]	0.7	0.05 ^{EC}
Tl	205	0.09 ± 0.06 (b)	0.24 ± 0.08 (a)	0.24 ± 0.09 (a)			0.53^{WR}
Pb	208	6.2 ± 3.6 (b)	10.8 ± 3.4 (a)	10.6 ± 3.4 (a)	47	112	46^{AR}
Th	232	4.5 ± 2.0 (b)	6.8 ± 1.5 (a)	5.9 ± 1.7 (a)			15^{AR}
U	238	1.06 ± 0.53 (b)	1.50 ± 0.37 (a)	1.04 ± 0.32 (b)			2.8^{AR}

Classes a, b, c (in brackets) according to the LSD test at the 95% confidence level, [#]t = value is for total of all chemical forms.

[†] From Macdonald et al. (1996) and adopted by US-EPA (1996); ERL value represents the lower 10th-percentile concentration associated with observation of biological effects, and PEL is the probable effects level.

[&] For Arsenic III.

[#] Chromium III.

[¶] Mercury inorganic.

[‡] Reference values for suspended sediments in African rivers (AR) or world rivers (WR), both from Viers et al. (2009), and in the Earth's crust (EC), from Rudnick and Gao (2003).

[§] Concentrations given in % and estimated from the count ratio with respect to the CRM IAEA-405.

[‖] Semi-quantitative concentrations estimated from the spectra and scaled by the known concentration in the CRM IAEA-405.

[*] Only four values over the MDL.

well as analysis and laboratory reagent blank checking (Creed et al., 1994).

Method detection limits were determined from reagent blanks by using the US-EPA 200.8 definitions (Enamorado-Báez et al., 2013). Each reagent blank was prepared using the same experimental procedure and reagents than the unknown samples. Results are shown in Table 1, and they compare well with those reported in similar studies involving acid-digestion of biological, soil and sediment samples (Enamorado-Báez et al., 2013, 2014).

Table 1 also reports results of the analysis of three full analytical replicates of the CRM IAEA-405, following the sample preparation described above. The percentage of recovery (Table 1) ranged from 53% (for V) to 104% (for Mn), with an average value of 83%. As expected, the acid digestion of soils with US-EPA method 3051A provides a pseudo-total recovery. It is worth noting that the adopted criterion for this work pursuits measuring the acid-digested (leachable) fraction of trace-elements in the bulk sediment, instead of getting a 100% of recovery (see Subsection 2.2). The reported uncertainties for recoveries (Table 1) account for the propagated errors from the standard deviation of the mean (of the three independent measurements) and the uncertainties provided for the reference and/or informative values.

The relative standard deviation corresponding to the three main runs of each measurement was typically under 2% for all the analytes. Concerning reproducibility of analysis, the relative standard deviation of the three analytical replicates of the CRM sample was 9 ± 4% (mean and standard deviation), while it was of 5 ± 4% for the three duplicated samples included within the main experiment.

In the reagent blanks, when treated as unknown samples with subtraction of the calibration blank, none of the elements was found over the method detection limits. Recovery of internal standards decreased monotonically throughout the experiment up to ~70% of their initial values, being this usual for ICP-MS analysis (Enamorado-Báez et al., 2013, 2014, 2015).

2.4. Granulometric analysis of sediments from the Ankobra estuary

In the present work, particle size distributions have been studied for a set of samples distributed along the Ankobra estuary (Fig. 2). Oven-dried samples were gently disaggregated using an agate mortar and then passed through a sieving column with mesh sizes of 2500, 1000, 100, 80, 63, 52, 45, 32 and 25 μm. The cumulative percentages at each diameter level were fitted by a Rosin-Rammler particle-size distribution (Vesilind, 1980) allowing for the estimation of mean and modal values.

2.5. Data treatment and statistical analysis

Statistical analysis was performed by using Statgraphics Centurion XVI.II software. After Kolmogorov-Smirnov normality tests, we performed ANOVA and pos-hoc mean comparison by Least Significant Difference (LSD) tests at 95% confidence level (CL) to assess differences between estuaries, and multivariate analysis for computation of the correlation matrices. Principal component analysis (PCA) was conducted with the above software for provenance studies and elemental associations. Measured concentrations corrected by digestion yields

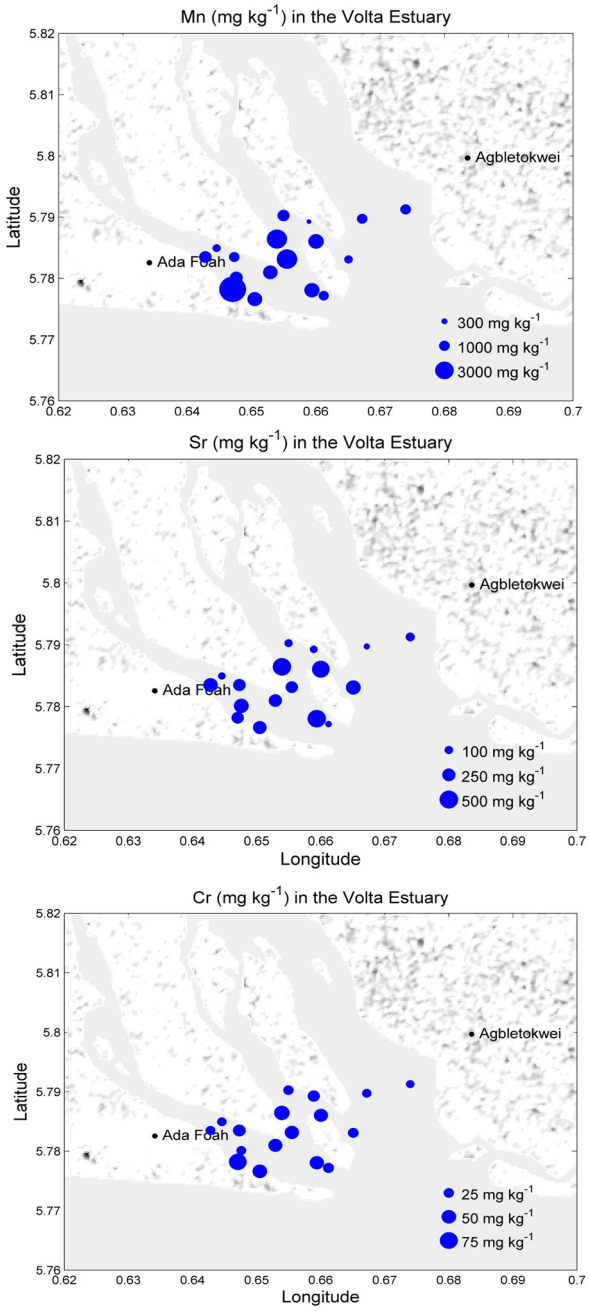

Fig. 4. Maps with the spatial distributions of concentrations of Mn, Sr and Cr in the Volta estuary. Digital terrain elevations with 1 arc-second spatial resolution have been taken from the Global Multi-resolution Terrain Elevation Data 2010 (GMTED2010) from the U.S. Geological Survey (USGS, https://lta.cr.usgs.gov/GMTED2010). Concentrations are proportional to the area of the circles, and the used scale is indicated.

were compared against the ERL and PEL values compiled by NOAA (2008). For those elements with mean values surpassing ERL, the frequency distributions for their natural logarithms were computed with Statgraphics and fitted to normal/lognormal distributions after Kolmogorov-Smirnov tests. This allowed for estimating continuous cumulative probability distributions and then the probability of surpassing the PEL values.

The geoaccumulation index (I_{geo}) and the enrichment factor (EF) were calculated. I_{geo} is a quantitative measure used in the scientific literature (Muller, 1969; Kumar and Edward, 2009; Magesh et al., 2011) of the extent of contamination in aquatic sediments:

$$I_{geo} = \log_2\left(\frac{C_n}{1.5 \cdot B_n}\right) \quad (1)$$

where C_n is the concentration of the studied elements in the sediment and B_n is the corresponding value for their geochemical background.

The enrichment factor (EF) is an estimate of the anthropogenic influence on sediments which uses a normalization element, X (Loring and Rantala, 1992):

$$EF = \frac{C_a \cdot X_b}{C_b \cdot X_a}, \quad (2)$$

where C_a and C_b are the examined metal content in the sample and the background reference respectively, and X_a and X_b are the content of the normalization element in the sample and the background reference, respectively. A review of useful normalization elements can be seen in Loring and Rantala (1992).

The spatial distributions of some relevant elements have been drawn using MATLAB software and the digital terrain elevations with 1 arc-second spatial resolution from the Global Multi-resolution Terrain Elevation Data 2010 from the U.S. Geological Survey (USGS, https://lta.cr.usgs.gov/GMTED2010).

3. Results and discussion

3.1. Granulometric characterization of samples from the Ankobra estuary

The Rosin-Rammler particle size distributions for sediment samples from the Ankobra estuary (Fig. 3) led to mean grain sizes of 77.6, 86.8, 91.4 and 78.0 μm, with modal values of 70, 91, 96 and 76 μm for sediment samples SA-1 to SA-4, respectively (see sampling sites in Fig. 2). Discussion on the implications of granulometry will be readdressed in Subsection 3.6.

3.2. Multielemental analyses

Results from the multielemental analyses of the surficial sediment samples in the three studied estuaries are summarized in Table 2, along with reference values for suspended sediments in African rivers, when available, or in World rivers (data from Viers et al., 2009), as the best available reference for comparison. When not reported in the previous reference, values for the Earth's crust (Rudnick and Gao, 2003) were provided. Table 2 also includes the ERL and PEL limits adopted by US-EPA (1996), based on the studies by Macdonald et al. (1996).

In all the cases data surpassed the Kolmogorov-Smirnov normality test, but for Cd in the Volta estuary (because a single influencing data). For comparison of measured values in Table 2 (pseudo-total digestion) against the reference ones and the ERL and PEL limits (ascribed to total digestion), the digestion yields must be taken into account (those reported in Table 1 can be used only as a gross estimate). It is worth noting that the reference levels from suspended sediments in African or World rivers will be used only as a first screening step to test the reliability of the Volta estuary as local reference site for the present study. Then, the subsequent comparisons will involve these local reference values and the same digestion procedure.

Overall, the measured concentrations were in the same order of magnitude than the reference values from Table 2. Exception was Ti, with measured concentrations being one order of magnitude below the reference values. This can be explained, at least partially, by a very low digestion yield in agreement with Enamorado-Báez et al. (2014) who reported 30% recovery for a soil reference material using a similar digestion method. Selenium was under the MDL in the three estuaries.

The following set of elements showed similar concentrations in the Pra and Ankobra estuaries, but with significantly higher values than in the Volta estuary (Table 2, LSD test): Be, Al, Fe, Co, Ni, Cu, Zn, Mo, Ag, Cd, Cs, Ba, Tl, Pb and Th (for Cd the transformation 1/X was applied in the statistical analysis). The gradation Ankobra > Pra > Volta was

Table 3
Reference levels ($mg \cdot kg^{-1}$ unless specified otherwise) from the Volta estuary ($n = 14$), and estimated geoaccumulation indexes I_{geo} and enrichment factors (EF) for the Pra ($n = 16$) and Ankobra ($n = 17$) estuaries, in Ghana. EF values are estimated for two normalization elements (Al and Fe). Values marked in bold indicate distinguishable levels of contamination (see text).

Element	Reference levels (Volta Estuary)	I_{geo}		EF (Al)		EF (Fe)	
		Pra	Ankobra	Pra	Ankobra	Pra	Ankobra
Be	0.54 ± 0.06	0.2 (−1.0, 0.9)	0.1 (−2.5, 0.8)	0.77 ± 0.05	0.78 ± 0.03	1.04 ± 0.03	1.06 ± 0.03
B	4.1 ± 0.6	−1.0 (−2.4, 0.3)	−0.9 (−1.7, −0.1)	0.41 ± 0.07	0.51 ± 0.13	0.50 ± 0.05	0.58 ± 0.06
Al[a]	3.3 ± 0.5	0.6 (−1.3, 1.7)	0.4 (−2.8, 1.2)			1.43 ± 0.11	1.40 ± 0.07
Ti	342 ± 29	−0.4 (−1.5, 0.2)	−0.8 (−1.9, −0.3)	0.54 ± 0.04	0.51 ± 0.10	0.72 ± 0.05	0.61 ± 0.05
V	18[b]	1.7 (0.3, 2.6)	2.7 (2.3, 3.0)	0.35 ± 0.02	1.2 ± 0.4	3.1 ± 0.2	7.6 ± 1.2
Cr	31 ± 3	0.8 (−0.6, 1.6)	1.2 (−1.3, 1.9)	1.16 ± 0.05	1.74 ± 0.08	1.58 ± 0.01	**2.35** ± 0.09
Mn	1180 ± 160	−3.0 (−4.0, −2.0)	−2.8 (−3.8, −2.1)	0.09 ± 0.01	0.13 ± 0.03	0.13 ± 0.01	0.16 ± 0.02
Fe[a]	2.5 ± 0.2	0.1 (−0.8, 0.7)	0.0 (−2.3, 0.6)	0.77 ± 0.07	0.77 ± 0.07		
Co	6.2 ± 0.6	0.7 (−0.4, 1.2)	0.4 (−1.5, 1.0)	1.15 ± 0.10	1.07 ± 0.11	1.51 ± 0.06	1.38 ± 0.04
Ni	10.0 ± 1.1	0.6 (−0.8, 1.3)	0.6 (−1.9, 1.3)	1.03 ± 0.05	1.14 ± 0.06	1.39 ± 0.05	1.53 ± 0.03
Cu	5.0 ± 0.8	**1.6** (0.2, 2.1)	**1.5** (−1.2, 2.2)	**2.07** ± 0.15	**2.14** ± 0.09	**2.75** ± 0.10	**2.90** ± 0.08
Zn	17.0 ± 1.9	0.9 (0.0, 1.5	0.9 (−1.0, 1.5)	1.36 ± 0.12	1.50 ± 0.14	1.78 ± 0.04	1.93 ± 0.03
As	5.0 ± 0.7	**1.5** (−0.1, 2.3)	**2.6** (1.0, 3.1)	**1.95** ± 0.15	**5.1** ± 0.7	**2.64** ± 0.15	**6.4** ± 0.3
Sr	220 ± 40	−3.0 (−4.0, −1.7)	−1.5 (−3.5, −0.9)	0.10 ± 0.02	0.27 ± 0.03	0.13 ± 0.02	0.35 ± 0.01
Mo	0.24 ± 0.07	0.5 (−0.9, 1.8)	0.8 (−1.2, 1.3)	1.11 ± 0.14	1.34 ± 0.13	1.43 ± 0.14	1.73 ± 0.03
Ag	0.023 ± 0.004	**1.5** (0.2, 2.1)	**1.8** (0.16, 2.4)	**2.01** ± 0.14	**4.3** ± 2.1	**2.69** ± 0.11	**4.1** ± 1.1
Cd	0.029 ± 0.004[c]	**1.0** (0.4, 1.7)	0.5 (−2.0, 1.1)	1.45 ± 0.17	1.12 ± 0.11	1.83 ± 0.09	1.47 ± 0.09
Sb	0.23 ± 0.03	0.4 (−0.6, 0.8)	**1.5** (0.7, 2.0)	0.99 ± 0.11	**2.7** ± 0.6	1.25 ± 0.07	**3.1** ± 0.4
Cs	0.61 ± 0.11	**1.4** (0.1, 2.1)	**1.2** (−1.9, 2.0)	1.87 ± 0.11	1.72 ± 0.03	**2.51** ± 0.09	**2.38** ± 0.11
Ba	30 ± 4	0.6 (−1.2, 1.7)	0.9 (−2.3, 1.8)	1.08 ± 0.05	1.41 ± 0.02	1.53 ± 0.12	1.95 ± 0.09
Tl	0.07 ± 0.01	1.0 (0.0, 1.7)	0.9 (−1.8, 1.7)	1.41 ± 0.10	1.40 ± 0.04	1.88 ± 0.05	1.92 ± 0.07
Pb	5.1 ± 0.7	0.4 (−0.7, 1.0)	0.3 (−2.0, 1.0)	0.94 ± 0.07	0.97 ± 0.06	1.26 ± 0.04	1.29 ± 0.02
Th	4.0 ± 0.5	0.1 (−0.6, 0.6)	−0.1 (−2.0, 0.4)	0.83 ± 0.13	0.71 ± 0.07	1.04 ± 0.06	0.91 ± 0.01
U	0.9 ± 0.1	0.1 (−0.5, 0.8)	−0.5 (−2.8, 0.1)	0.86 ± 0.17	0.53 ± 0.03	1.03 ± 0.09	0.71 ± 0.01

Reference levels are mean values and the standard deviation of the mean (data from Volta estuary after excluding sites 5, 8 and 9 in Fig. 2).
For I_{geo}, values are provided as the arithmetic mean and the range.
For EF, values are provided as the mean and the standard deviation of the mean.
[a] Concentrations given in %.
[b] Only two values over the MDL.
[c] Excluding data from sampling site number 10 (Fig. 2).

found for V, Cr, As, Sb, and Hg, from which As and Hg are the elements typically associated to the major gold mining impacts (Fashola et al., 2016). The concentrations of B, Mn and Sr were higher in the Volta estuary while similar in the Pra and Ankobra. In the case of Mn, its mean concentration in the Volta was seven times higher than those for the other estuaries. The concentrations of U (and Ti) were significantly higher in the Pra than in the other two estuaries.

3.3. The Volta estuary as a local reference site

The geoaccumulation index has been estimated for all the elements fully quantified in the Volta estuary by using the reference levels provided in Table 2 and, as a first estimate, correcting the measured pseudo-total concentrations by the digestions yields provided in Table 1. I_{geo} was negative in all the cases, indicating the absence of contamination, by except Mn, Sr, and Cd.

The reference value used for Mn ($1478\ mg \cdot kg^{-1}$) is higher than that for the Earth's crust ($720\ mg \cdot kg^{-1}$). For Mn, I_{geo} took negative values in all the sampling sites but at the sampling stations 5, 8 and 9 (see Fig. 2), with values of 1.47, 0.70 and 0.68, respectively. The spatial distribution of Mn concentrations in sediments from the Volta estuary (Fig. 4) is compatible with the presence of local sources of contamination. Aliquots of the bulk samples used in this study were preserved for control purposes. In sample number 5, near the Ada-Foah urban area, we found an oxidized metallic piece of about 1.5 cm size. Thus, the urban wastes may impact this area, which showed the highest concentrations for Be, B, al, Ti, Cr, Mn, Fe, Co, Ni, Cu, Zn, Ag, Cs, Ba, Tl, Pb and U. Sampling sites 7 and 8 were near the effluent draining out from the major estuarine island, with agriculture lands, and they may be enriched in Mn. For Cd, despite the low reference level (Table 2), I_{geo} was positive (0.1) only for the sampling site number 10, around the outlet of a small water stream. Thus, no significant contamination can be concluded for Cd.

For Sr, I_{geo} was positive in seven cases, with the highest value (0.93) found at site n. 9 (Fig. 2) what, according to the interpretation of I_{geo}, corresponds to uncontaminated to moderately contaminated sediments. The screening reference level used for Sr (Table 2) is usual for suspended river sediments (Viers et al., 2009), but smaller than its mean concentration in the Earth's crust ($320\ mg \cdot kg^{-1}$). Fig. 4 also plots the map with the spatial distribution of concentrations for Sr and Cr in the Volta estuary. Chromium, with a mean value of −2.1 for I_{geo}, is used for the sake of comparison with a non-enriched element. Despite the great spatial variability, no particular contamination patterns can be inferred.

Table 3 reports the mean values (and the standard deviation of the mean) for the measured concentrations of the studied elements in the Volta Estuary, after excluding sampling sites 5, 8 and 9, where possible anthropogenic impacts are supposed to occur as mentioned above. They depict a relatively pristine scenario, with overall concentrations lower than those reported for suspended sediments in African and World rivers, but for As, Mn and Sr, which showed similar or slightly higher values. This can be considered as the characteristic lithological fingerprint of the Volta estuary, whose upper and medium basin is dominated by sandstones, mudstones, slates, carbonates and mafic rocks (Petersson et al., 2018). Thus, concentrations reported in Table 3 reasonably meet the conditions by Loring and Rantala (1992) for serving as reference levels for the study of the Ankobra and Pra estuaries.

3.4. Enrichment factors and geoaccumulation indexes

Geoaccumulation index and enrichment factors have been estimated at each sampling point using as background the reference levels for the Volta estuary. Results are reported in Table 3. The mean value of I_{geo} was > 2 (moderated to heavily contaminated) only for As in the

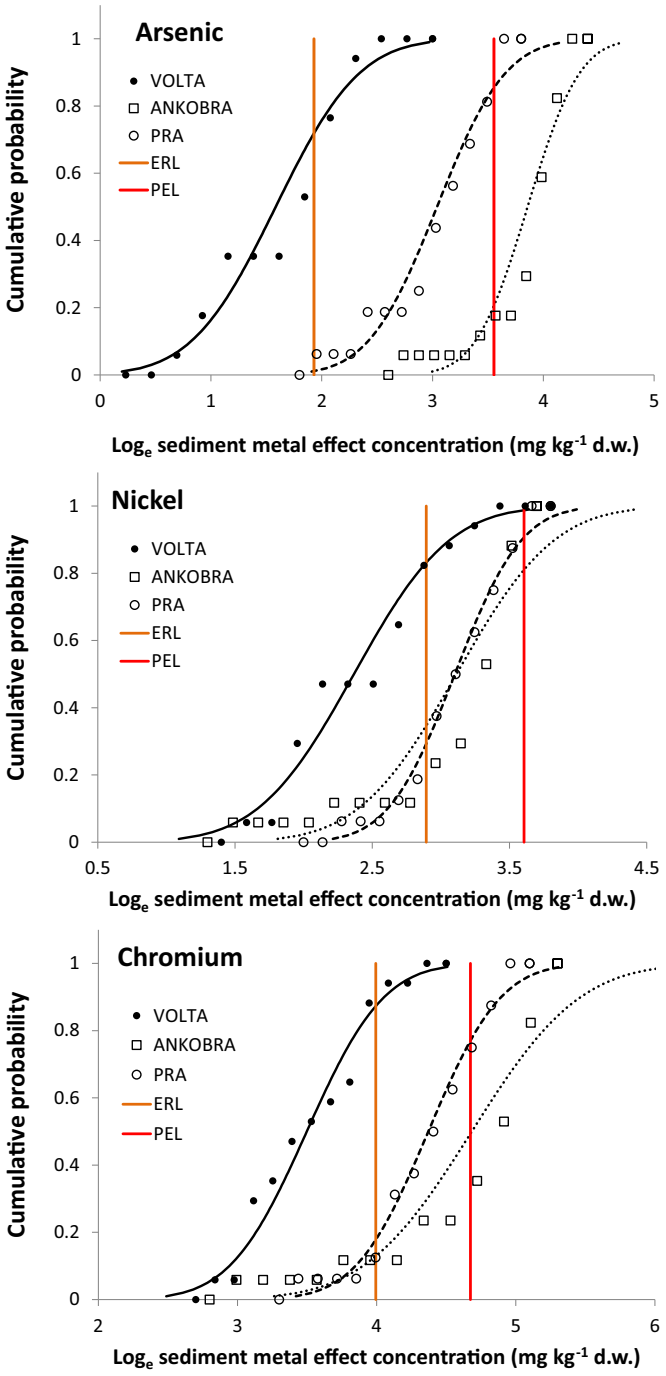

Fig. 5. Cumulative probability distributions for the natural logarithm of the concentrations of As, Ni and Cr in the set of samples from the Volta, Pra and Ankobra estuaries. Continuous lines are the fitted normal distributions (which showed the best performance after a Kolmogorov-Smirnov test). Their respective ERL and PEL values (Table 2), corrected by the digestion yields reported in Table 1, are also depicted for the sake of comparison.

Ankobra estuary. Moderate contamination levels ($1 < I_{geo} < 2$) were found for Ag, Cu, Sb, Cr and Cs in the Ankobra estuary, and for As, Cu, Ag, and Cs in the Pra estuary. Results for V cannot be considered as confident enough, since its reference level in the Volta was determined only from two measurements above the MDL.

The role of Al as a normalization element is that of a chemical tracer of Al-silicates, particularly the clay minerals (Loring and Rantala, 1992), which in this study (with pseudo-total digestions) limits to their method-extractable fraction. This normalization discards spurious enrichments merely due to an increase in the proportion of Al-silicates. When using Al for normalization (Eq. (2)), only the following elements reached an EF over 2 (moderate enrichment): As, Ag, Sb and Cu in the Ankobra estuary; and Cu, and Ag, in the Pra estuary, where EF for As was around 2.

Iron serves a chemical tracer for Fe-rich clay minerals (Loring and Rantala, 1992). Its use as normalization element led to EF values (Table 3) over 2 for As, Ag, Sb, Cu, Cs and Cr in the Ankobra estuary, and the same in the Pra, but for Sb and Cr. It is worth noting that, although poorly confident as above commented, the high EF(Fe) for V in both estuaries seems to be related to a higher proportion of Al-silicates, as inferred from the low EF(Al) value. The same is true, to some extent, for Cs and Cr. Only three elements fulfilled all the criteria for moderate to significant enrichment in both estuaries: As, Ag and Cu. Contamination levels were higher in the Ankobra estuary, where Sb also met the above criteria. According to the EF interpretation, these elements cannot be associated to the same class of Fe-rich minerals existing in the Volta estuary, which is compatible with their association to mining tailing particles, such as arsenopyrite (for the case of As). Discussion will be readdressed after statistical analysis.

3.5. ERL and PEL limits

These screening values account for the biological effects of some elements on reference biotic communities. Bu the values of Table 2 are not site specific, thus their use only provides a preliminary evaluation of potential hazards which merit a more detailed study. The ERL value for Cr, Ni, As and Hg was surpassed by the mean concentrations found in both the Pra and Ankobra estuaries. The PEL value was surpassed only by Cr and As in the Ankobra estuary (Table 2). For Cr, Ni, and As, with fully quantitative determinations, the natural logarithm of their concentrations showed distributions compatible with normal ones (after a Kolmogorov-Smirnov test), and their respective cumulative probability distributions are shown in Fig. 5 with the corresponding fitted curves. The ERL and PEL values, corrected by the digestion yields reported in Table 1 (as a first estimate) are also depicted for the sake of comparison. In the Ankobra estuary, the probability of surpassing the PEL value for As was of 77%, while this probability was only of 13% and 0% for the Pra and Volta estuaries, respectively, as deduced from Fig. 5. For Ni, the probability of exceeding the PEL value was of 27%, 10% and 1% for the Ankobra, Pra and Volta estuaries, respectively. Finally, for Cr, the probability of exceeding the PEL value was of 50%, 23% and 0% for the Ankobra, Pra and Volta estuaries, respectively.

Attending to the potential biological effects (estimated through the indexes ERL and PEL), As seems to pose the major concern, particularly in the Ankobra estuary. Nevertheless, the quantification of its potential effects to the environment and human health is not straightforward due to its co-occurrence with other harmful elements (Sobrino-Figueroa et al., 2015). An important exposure pathway can be the bioaccumulation of As in fish and invertebrates (Meador et al., 2004). The bioaccumulation factors may be particularly high for some species of bivalves, such as the soft-shell clams (Doe et al., 2017).

3.6. Spatial distribution maps

Maps with the spatial distribution of I_{geo} (related to concentrations by Eq. (1)) have been depicted for As (Fig. 6) and Ag (Fig. 7) in the Pra and Ankobra estuaries. High concentrations are found at most of the sampling sites. This seems consistent with non-localized sources for these elements. The lack of industrial activities in the rural south-western region of Ghana drained by the Pra and Ankobra rivers makes small-scale gold mining the most likely source of As enrichment in the studied estuarine sediments (Donkor et al., 2005).

It is worth noting that in the Ankobra estuary, coarser sediments were found along the sand ramp, between the river mouth and the freshwater limit (see site description and Fig. 3). However, this did not

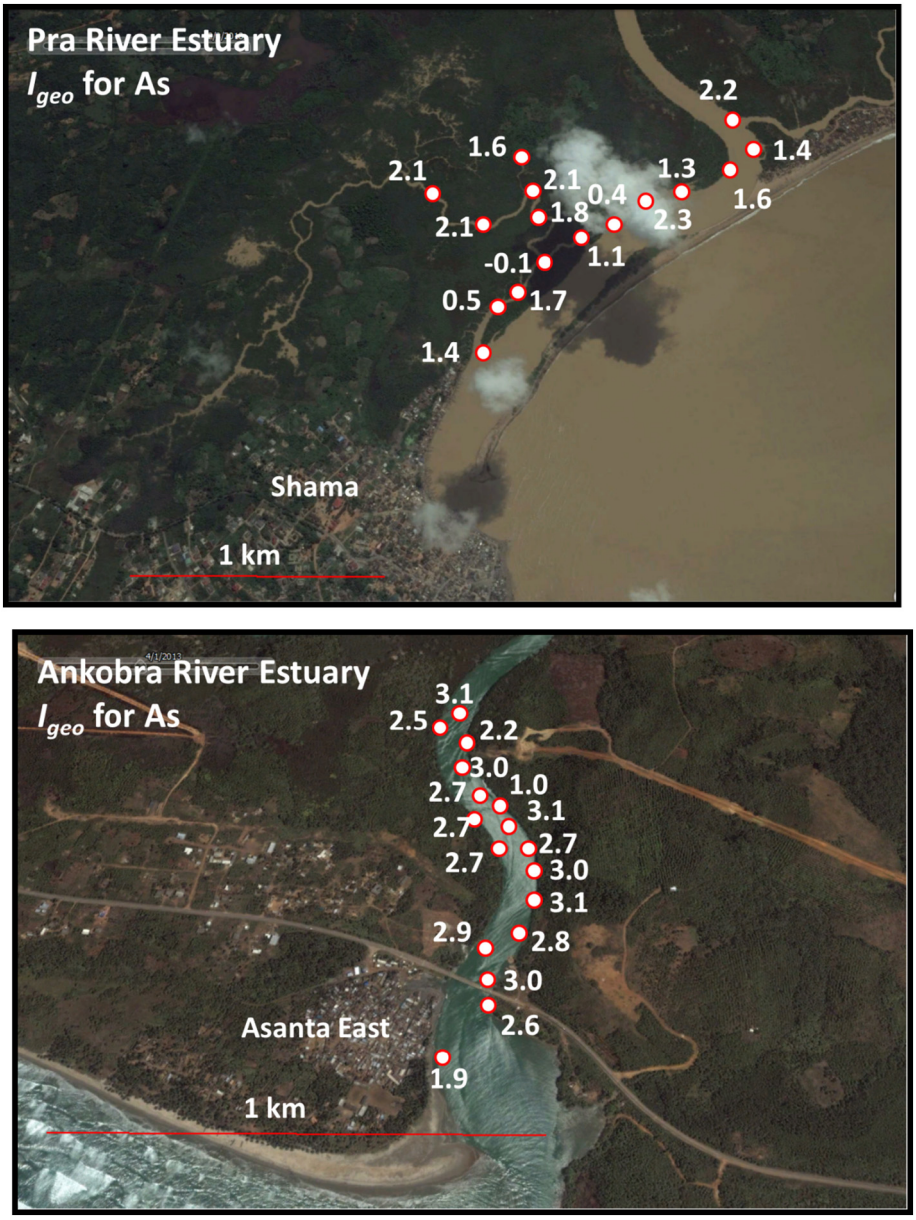

Fig. 6. Spatial distribution of I_{geo} (related to concentrations and with reference levels from Table 3) for As in the Pra and Ankobra estuaries (background image taken from Google Earth).

result in lower values for As concentrations (Fig. 6), as it could be expected if the dominant process was its uptake from the water column by the settling particulate matter (Abril, 1998; Barros et al., 2004). This suggests that As accumulation was likely dominated by the settling of suspended particles with provenance in the mining tailings. As the bulk As concentrations are one order of magnitude lower that those reported in gold mining tailings from Obuasi, Ghana (range 452 to 1572 $mg{\cdot}kg^{-1}$, after Bempah et al., 2013), the above mass flow, with a high As content, must be mixed with other terrigenous mass flows bearing lower concentrations of As. Thus, zones with higher As concentration should reveal where the highest amount of sediments from mining tailings were accumulated and consequently the zones in each estuary which were more impacted by mining activity.

Since gold mining activities in Ghana take place primarily in the river banks and flood plains, during the raining season high amounts of particles eroded from soils and mine tailings are expected to be carried into waterways by runoffs. Thus, the levels of all examined trace metals in sediments from the Pra River increased from the dry to the rainy season (Donkor et al., 2005). The high turbidity of waters in the Pra and Ankobra rivers (as it can be seen in available aerial photographs) would be likely associated to these inputs of matter. This would result in high sediment accumulation rates (SAR), as shown by Klubi et al. (2017).

3.7. Correlation and PCA analysis

Table 4 shows the Pearson correlation coefficient matrixes based in complete-linkage for elements in the sediments from the Volta (Table 4a), Pra (Table 4b) and Ankobra (Table 4c) estuaries, respectively. They exclude Se (under MDL) and Hg (semi-quantitative determination).

In the Volta estuary, elements were correlated at a 95% CL or higher, by except Cd (with all the elements) and few cases of (Sr, Mn), (Sr, Cu), (Be, Ba), (Be, Th), (As, Th), and (As, U). In the Pra estuary, most of the elements were also highly correlated among them (Table 4b); here the elements with a differential pattern were Sr (uncorrelated with all the others), B and U (uncorrelated with 14 and 8

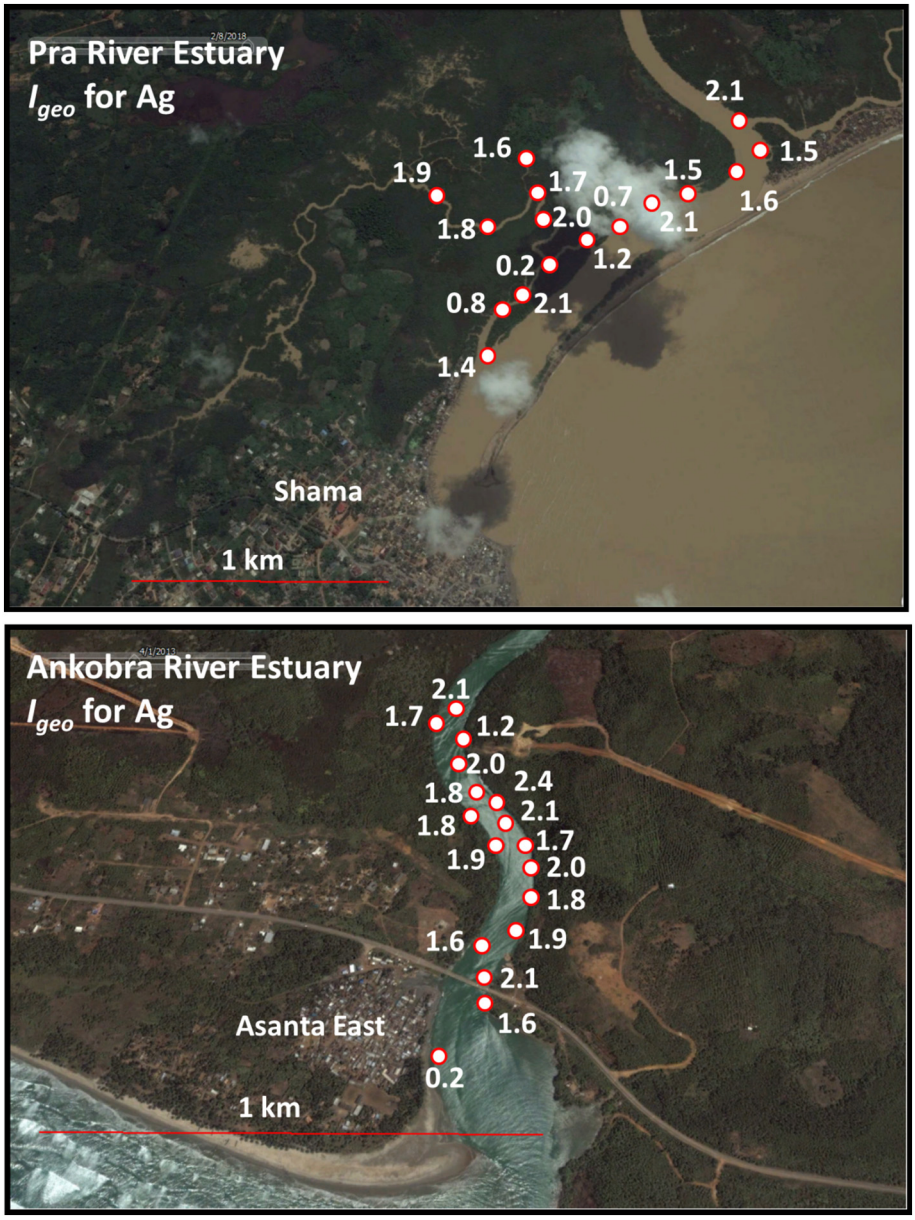

Fig. 7. Spatial distribution of I_{geo} (related to concentrations and with reference levels from Table 3) for As in the Pra and Ankobra estuaries (background image taken from Google Earth).

elements, respectively). In the Ankobra estuary, the elements with a distinct behaviour were Ag, Mn and Sb. The above correlations must be understood in the frame of the used acid-digestion method. They are consistent with the studies by Donkor et al. (2005), who reported strong ($r > 0.81$) and significant ($p < 0.01$) correlations between Al and Fe, Cu, Ni, V, Cr, and Zn in sediments from the Pra River during the dry season. These authors also found a lack of relationship between the organic matter content and all the analysed metals; thus, these metals must be mostly associated with the inorganic fraction of sediments.

Arsenic provenance is most likely associated with the gold mining tailings where this element is present as arsenopyrite, realgar and orpiment (Fashola et al., 2016). Sulphur has not been analysed in this work, but special mention merits the coexistence of As and Fe in arsenopyrites. Thus, the high Fe concentrations found in sediments from Ankobra and Pra estuaries with respect to the Volta (Table 2) are also likely related to the gold mining impacts.

Slopes from the linear regressions can provide additional insights. Limiting the discussion to the set of contaminants identified by I_{geo} and EF, for Ankobra and Pra the slopes of As, Cu and Ag vs Fe concentrations were significantly higher than those for the Volta reference estuary (Fig. 8). The same is true for Cr (not shown). This indicates a different nature for the associations of these elements with Fe, in agreement with the EF(Al) and EF(Fe) analysis and with the hypothesis of a direct contribution of particles from the gold mining tailings to the Ankobra and Pra sediments, particularly arsenopyrites. In the case of Ag, its presence in the gold mining tailings in Ghana has not been previously reported. Its known mineral forms are not associated to Fe, but mostly to S, Cl and As. Thus, the Ag correlation with Fe would indicate the common fate of tailing particles with a composite mineralogy.

A more comprehensive view of the provenance of trace elements could be achieved through PCA analysis (Zitko, 1994). The study comprised the 50 sediment samples and the 23 trace elements fully quantified in all the samples over their respective MDLs. The eigenvalues and percentage of variance (in parentheses) for the first three components were 14.96 (65.0%), 3.47 (15.1%) and 1.34 (5.8%),

Table 4a
Pearson correlation coefficient matrix based in complete-linkage for elements in the sediments from the Volta Estuary ($n = 17$): $|r| > 0.414$, $p < 0.05$; $|r| > 0.482$, $p < 0.025$; $|r| > 0.558$, $p < 0.01$; $|r| > 0.606$, $p < 0.005$.

	Be	B	Al	Ti	Cr	Mn	Fe	Co	Ni	Cu	Zn	As	Sr	Mo	Ag	Cd	Sb	Cs	Ba	Tl	Pb	Th	U
Be	1	**0.969**	**0.985**	**0.937**	**0.966**	**0.835**	**0.986**	**0.960**	**0.976**	**0.950**	**0.989**	**0.857**	**0.643**	**0.703**	**0.974**	−0.086	**0.828**	**0.975**	−0.086	**0.828**	**0.975**	−0.086	**0.828**
B		1	**0.933**	**0.881**	**0.933**	**0.881**	**0.914**	**0.841**	**0.965**	**0.881**	**0.980**	**0.916**	**0.734**	**0.527**	**0.918**	−0.085	**0.814**	**0.911**	**0.918**	**0.920**	**0.959**	**0.589**	**0.755**
Al			1	**0.923**	**0.964**	**0.833**	**0.958**	**0.966**	**0.994**	**0.978**	**0.971**	**0.776**	**0.545**	**0.751**	**0.988**	−0.028	**0.823**	**0.994**	**0.975**	**0.996**	**0.974**	**0.658**	**0.902**
Ti				1	**0.905**	**0.694**	**0.913**	**0.858**	**0.893**	**0.873**	**0.910**	**0.813**	**0.640**	**0.762**	**0.919**	−0.060	**0.753**	**0.911**	**0.879**	**0.913**	**0.911**	**0.679**	**0.837**
Cr					1	**0.838**	**0.976**	**0.957**	**0.970**	**0.968**	**0.962**	**0.736**	**0.481**	**0.692**	**0.974**	−0.030	**0.887**	**0.967**	**0.941**	**0.964**	**0.985**	**0.679**	**0.912**
Mn						1	**0.870**	**0.931**	**0.863**	**0.853**	**0.884**	**0.622**	0.364	0.404	**0.850**	0.045	**0.608**	**0.833**	**0.900**	**0.825**	**0.863**	**0.565**	**0.731**
Fe							1	**0.963**	**0.958**	**0.936**	**0.987**	**0.840**	**0.615**	**0.630**	**0.959**	−0.080	**0.836**	**0.949**	**0.955**	**0.950**	**0.984**	**0.629**	**0.854**
Co								1	**0.982**	**0.976**	**0.974**	**0.721**	**0.452**	**0.640**	**0.975**	−0.041	**0.768**	**0.970**	**0.974**	**0.965**	**0.964**	**0.628**	**0.902**
Ni									1	**0.992**	**0.971**	**0.735**	**0.480**	**0.733**	**0.993**	−0.024	**0.826**	**0.996**	**0.977**	**0.994**	**0.973**	**0.640**	**0.921**
Cu										1	**0.948**	**0.662**	0.386	**0.747**	**0.990**	−0.011	**0.822**	**0.991**	**0.958**	**0.986**	**0.958**	**0.645**	**0.951**
Zn											1	**0.846**	**0.623**	**0.624**	**0.969**	−0.062	**0.818**	**0.964**	**0.960**	**0.965**	**0.983**	**0.628**	**0.852**
As												1	**0.935**	**0.439**	**0.735**	−0.143	**0.668**	**0.733**	**0.751**	**0.753**	**0.797**	**0.443**	**0.535**
Sr													1	0.263	**0.477**	−0.165	**0.470**	**0.483**	**0.511**	**0.513**	**0.566**	0.290	0.246
Mo														1	**0.750**	−0.065	**0.539**	**0.771**	**0.691**	**0.772**	**0.637**	**0.439**	**0.821**
Ag															1	−0.021	**0.832**	**0.994**	**0.966**	**0.992**	**0.975**	**0.646**	**0.931**
Cd																1	−0.018	−0.035	0.022	−0.037	−0.052	−0.142	−0.133
Sb																	1	**0.817**	**0.750**	**0.825**	**0.881**	**0.579**	**0.741**
Cs																		1	**0.967**	**0.998**	**0.966**	**0.643**	**0.934**
Ba																			1	**0.969**	**0.952**	**0.613**	**0.858**
Tl																				1	**0.967**	**0.638**	**0.922**
Pb																					1	**0.683**	**0.869**
Th																						1	**0.650**
U																							1

Values marked in boldface are correlated at a 95% CL or higher.

Table 4b
Pearson correlation coefficient matrix based in complete-linkage for elements in the sediments from the Pra Estuary ($n = 16$): $|r| > 0.426$, $p < 0.05$; $|r| > 0.497$, $p < 0.025$; $|r| > 0.574$, $p < 0.01$; $|r| > 0.623$, $p < 0.005$.

	Be	B	Al	Ti	Cr	Mn	Fe	Co	Ni	Cu	Zn	As	Sr	Mo	Ag	Cd	Sb	Cs	Ba	Tl	Pb	Th	U
Be	1	0.391	**0.956**	**0.590**	**0.991**	**0.472**	**0.956**	**0.833**	**0.990**	**0.937**	**0.924**	**0.892**	0.253	**0.532**	**0.945**	**0.527**	**0.565**	**0.985**	**0.876**	**0.982**	**0.969**	**0.870**	**0.461**
B		1	0.230	−0.098	0.376	−0.353	**0.487**	0.057	0.417	0.374	**0.590**	0.281	0.201	**0.784**	0.411	**0.619**	0.260	**0.505**	−0.014	**0.533**	0.366	0.294	**0.807**
Al			1	**0.757**	**0.961**	**0.584**	**0.876**	**0.822**	**0.959**	**0.832**	**0.825**	**0.792**	0.342	0.303	**0.867**	**0.426**	**0.471**	**0.909**	**0.956**	**0.906**	**0.885**	**0.790**	0.284
Ti				1	**0.641**	**0.707**	**0.491**	**0.666**	**0.643**	**0.468**	**0.490**	0.389	0.273	−0.072	**0.523**	0.303	0.260	**0.492**	**0.808**	**0.492**	**0.482**	0.355	−0.174
Cr					1	**0.532**	**0.959**	**0.854**	**0.989**	**0.936**	**0.924**	**0.884**	0.244	**0.517**	**0.940**	**0.553**	**0.595**	**0.971**	**0.886**	**0.970**	**0.956**	**0.861**	**0.443**
Mn						1	0.418	**0.778**	**0.498**	**0.474**	0.425	**0.495**	0.119	−0.159	**0.514**	0.390	**0.524**	0.377	**0.751**	0.382	**0.481**	**0.463**	−0.162
Fe							1	**0.818**	**0.952**	**0.940**	**0.921**	**0.912**	0.242	**0.666**	**0.915**	**0.579**	**0.662**	**0.965**	**0.766**	**0.965**	**0.942**	**0.806**	**0.530**
Co								1	**0.856**	**0.889**	**0.810**	**0.840**	0.090	0.347	**0.890**	**0.596**	**0.755**	**0.795**	**0.876**	**0.787**	**0.872**	**0.744**	0.144
Ni									1	**0.934**	**0.943**	**0.872**	0.262	**0.533**	**0.959**	**0.591**	**0.608**	**0.980**	**0.883**	**0.979**	**0.960**	**0.837**	**0.437**
Cu										1	**0.934**	**0.938**	0.033	**0.658**	**0.968**	**0.604**	**0.742**	**0.943**	**0.774**	**0.934**	**0.977**	**0.863**	**0.456**
Zn											1	**0.848**	0.180	**0.691**	**0.965**	**0.783**	**0.685**	**0.951**	**0.732**	**0.958**	**0.936**	**0.816**	**0.588**
As												1	0.116	**0.634**	**0.914**	**0.502**	**0.728**	**0.896**	**0.742**	**0.893**	**0.945**	**0.852**	**0.426**
Sr													1	−0.020	0.131	0.089	−0.175	0.268	0.308	0.259	0.182	0.044	−0.087
Mo														1	**0.598**	**0.589**	**0.529**	**0.626**	0.104	**0.636**	**0.588**	**0.496**	**0.712**
Ag															1	**0.691**	**0.730**	**0.956**	**0.820**	**0.9560**	**0.980**	**0.867**	**0.460**
Cd																1	**0.648**	**0.580**	0.377	**0.618**	**0.571**	**0.510**	**0.558**
Sb																	1	**0.560**	**0.481**	**0.603**	**0.672**	**0.538**	0.346
Cs																		1	**0.806**	**0.996**	**0.975**	**0.849**	**0.525**
Ba																			1	**0.796**	**0.832**	**0.738**	0.072
Tl																				1	**0.966**	**0.863**	**0.572**
Pb																					1	**0.888**	**0.440**
Th																						1	0.577
U																							1

Values marked in boldface are correlated at a 95% CL or higher.

Table 4c
Pearson correlation coefficient matrix based in complete-linkage for elements in the sediments from the Ankobra Estuary ($n = 17$): $|r| > 0.414$, $p < 0.05$; $|r| > 0.482$, $p < 0.025$; $|r| > 0.558$, $p < 0.01$; $|r| > 0.606$, $p < 0.005$.

	Be	B	Al	Ti	Cr	Mn	Fe	Co	Ni	Cu	Zn	As	Sr	Mo	Ag	Cd	Sb	Cs	Ba	Tl	Pb	Th	U
Be	1	**0.839**	**0.992**	**0.759**	**0.988**	0.273	**0.988**	**0.920**	**0.995**	**0.984**	**0.987**	**0.833**	**0.985**	**0.973**	0.364	**0.716**	0.361	**0.995**	**0.984**	**0.996**	**0.992**	**0.990**	**0.982**
B		1	**0.847**	**0.524**	**0.833**	−0.128	**0.821**	**0.632**	**0.810**	**0.790**	**0.806**	**0.550**	**0.856**	**0.820**	**0.432**	0.353	0.175	**0.852**	**0.816**	**0.860**	**0.829**	**0.809**	**0.772**
Al			1	**0.794**	**0.987**	0.275	**0.978**	**0.898**	**0.987**	**0.967**	**0.970**	**0.804**	**0.989**	**0.951**	0.389	**0.678**	0.348	**0.988**	**0.993**	**0.993**	**0.980**	**0.975**	**0.968**
Ti				1	**0.778**	**0.640**	**0.720**	**0.780**	**0.779**	**0.735**	**0.741**	**0.778**	**0.748**	**0.666**	0.191	**0.737**	**0.506**	**0.718**	**0.838**	**0.737**	**0.732**	**0.716**	**0.777**
Cr					1	0.269	**0.972**	**0.908**	**0.988**	**0.974**	**0.981**	**0.841**	**0.970**	**0.958**	0.387	**0.699**	0.362	**0.980**	**0.980**	**0.986**	**0.979**	**0.974**	**0.967**
Mn						1	0.305	**0.574**	0.341	0.358	0.328	**0.622**	0.216	0.233	0.019	**0.784**	**0.618**	0.236	0.367	0.246	0.296	0.308	0.380
Fe							1	**0.935**	**0.989**	**0.993**	**0.989**	**0.844**	**0.973**	**0.980**	0.360	**0.734**	0.409	**0.990**	**0.971**	**0.990**	**0.997**	**0.996**	**0.984**
Co								1	**0.948**	**0.963**	**0.951**	**0.936**	**0.865**	**0.914**	0.323	**0.909**	**0.547**	**0.909**	**0.920**	**0.910**	**0.934**	**0.946**	**0.958**
Ni									1	**0.993**	**0.994**	**0.864**	**0.975**	**0.971**	0.364	**0.759**	0.398	**0.991**	**0.987**	**0.992**	**0.993**	**0.993**	**0.987**
Cu										1	**0.996**	**0.880**	**0.954**	**0.978**	0.361	**0.786**	**0.426**	**0.983**	**0.967**	**0.983**	**0.993**	**0.996**	**0.988**
Zn											1	**0.871**	**0.962**	**0.981**	0.321	**0.771**	**0.421**	**0.985**	**0.968**	**0.984**	**0.995**	**0.992**	**0.983**
As												1	**0.766**	**0.815**	0.269	**0.924**	**0.587**	**0.800**	**0.846**	**0.811**	**0.844**	**0.854**	**0.878**
Sr													1	**0.948**	0.320	**0.636**	0.300	**0.987**	**0.978**	**0.986**	**0.977**	**0.965**	**0.950**
Mo														1	0.295	**0.706**	0.430	**0.976**	**0.931**	**0.974**	**0.984**	**0.981**	**0.966**
Ag															1	0.162	−0.078	0.372	0.398	0.394	0.327	0.372	0.348
Cd																1	0.622	**0.684**	**0.732**	**0.688**	**0.736**	**0.751**	**0.790**
Sb																	1	0.333	0.377	0.348	**0.417**	0.402	**0.433**
Cs																		1	**0.976**	**0.998**	**0.993**	**0.991**	**0.972**
Ba																			1	**0.982**	**0.973**	**0.969**	**0.969**
Tl																				1	**0.992**	**0.990**	**0.974**
Pb																					1	**0.995**	**0.982**
Th																						1	**0.987**
U																							1

Values marked in boldface are correlated at a 95% CL or higher.

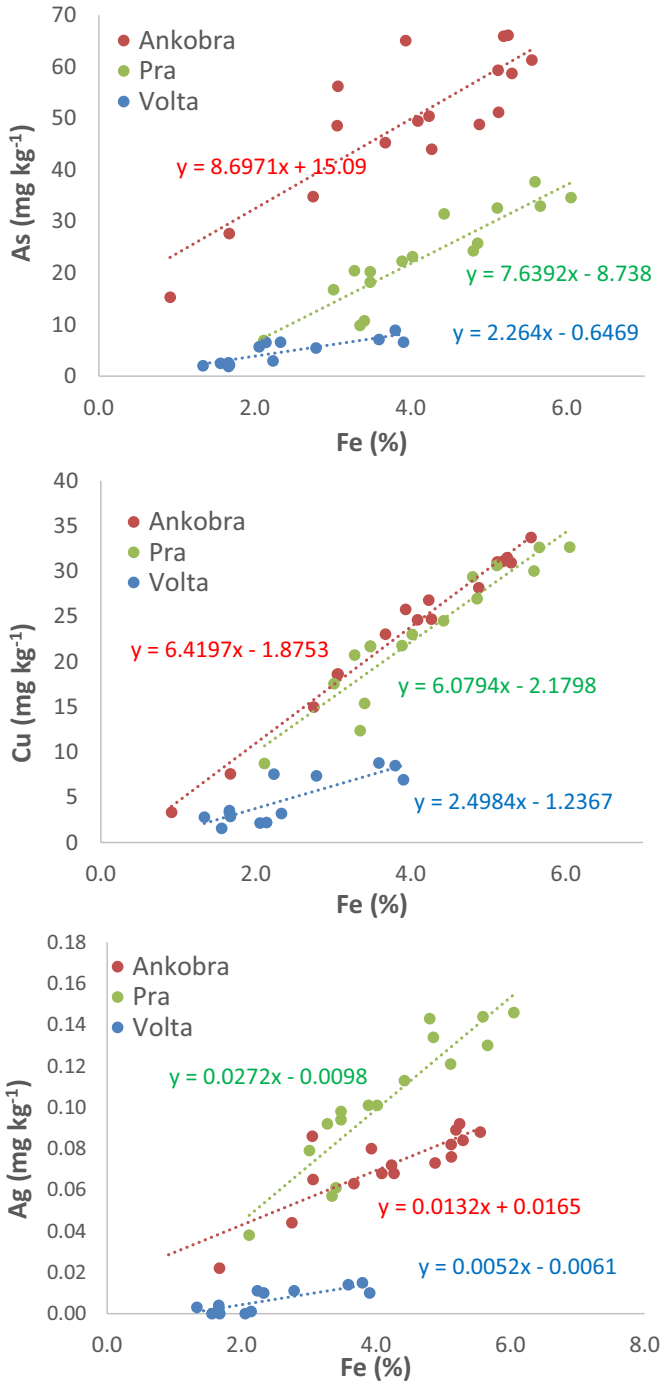

Fig. 8. Linear fits for As, Cu and Ag vs Fe concentrations in the Ankobra, Pra and Volta estuaries. The slopes for As and Cu were similar for Ankobra and Pra while higher than in the Volta at 95% confidence level. The gradation Pra > Ankobra > Volta applies for the slopes of Ag vs Fe.

respectively. The expressions for the two first components are:

F1 = 0.2467•Be + 0.0712•B + 0.2446•Al + 0.1154•Ti + 0.2402•Cr − 0.0367•Mn + 0.2440•Fe + 0.2424•Co + 0.2570•Ni + 0.2501•Cu + 0.2525•Zn + 0.1979•As − 0.0323•Sr + 0.2119•Mo + 0.2189•Ag + 0.0345•Cd + 0.1654•Sb + 0.2534•Cs + 0.2430•Ba + 0.2563•Tl + 0.2526•Pb + 0.2181•Th + 0.1714•U,

F2 = −0.1396•Be − 0.4534•B − 0.0867•Al − 0.3600•Ti + 0.1187•Cr − 0.4587•Mn − 0.1525•Fe0.0279•Co − 0.0124•Ni + 0.1185•Cu + 0.0729•Zn + 0.2485•As − 0.3765•Sr + 0.0224•Mo + 0.1636•Ag + 0.0309•Cd + 0.2405•Sb + 0.0442•Cs + 0.0352•Ba + 0.0188•Tl − 0.0824•Pb − 0.0969•Th − 0.2460•U,

where symbols for elements represent the standardized values for their respective concentrations.

Component F1 is characterized by a high positive contribution of most of the elements, particularly the group Fe, Co and Ni and Al. The elements As, Ag, Cd and Sb have similar coefficients for F1 and F2. Finally, F2 is characterized by a large negative contribution of Mn and Sr (which seem to represent the particular lithological fingerprint of the Volta estuary, as discussed in Subsection 3.3).

Fig. 9 plots the coordinates of each sediment sample in the (F1, F2) space. There are two well distinct clusters, the first one comprised by samples from the Volta and the second by samples of both Pra and Ankobra estuaries, showing these latest a slightly higher contribution from component F2. Sediments from the Volta tend to occupy the area of negative values for axis F2, which can be consistently explained by their higher Mn concentrations (Table 2). Thus, the lowest F2 coordinate corresponds to sampling point 5 in the Volta. This cluster also shows negative values for F1 coordinates.

When applying PCA analysis separately to each estuary, the component F1 is encountered in all the cases with only slight variations in the coefficients (with exception of positive coefficients for Mn and Sr in the Volta estuary, and for Sr in Ankobra). This principal component can be related to the bulk of the samples which share a similar elemental composition. Distinct fingerprints can be found in the second principal component. Thus, the second component in the Volta explains 6.4% of the variance and it is characterized by high positive contributions of As and Sr (both being correlated with $r = 0.935$; see Table 4a), and a third component, with 4.6% of the variance is mainly contributed by Mn and Cd. In the Ankobra estuary, the second principal component explains 9.7% of the variance and it is positively contributed by Mn, As, Ti, Cd, Sb and Co, with relatively high but negative coefficients for B and Ag. In the Pra estuary, the second principal component explains 13.8% of the variance with relatively high positive contributions from Ti, Mn, Co, Ba and Al, and negative of B and Mo. Consequently, the PCA results may be reflecting only the occurrence of different lithologies among the three studied areas.

All the above features are consistent with moderate impacts in the Ankobra and Pra estuaries due to gold mining activities and being associated to the transport and sedimentation of mining-tailing particles rather than to leaching processes from tailings dams. In these estuaries, a composite mass-flow feeds sediment accretion and it can explain the main features of the observed spatial distributions of As. This element is, from the set of fully-quantified analytes in this study, that of major concern, as shown in Fig. 5.

4. Conclusions

The mean concentrations of most of the studied trace elements were higher in the two gold-mining impacted estuaries (Pra and Ankobra) than in the Volta.

The application of I_{geo} with reference levels from literature served for stablishing as suitable local reference the concentrations measured in the Volta estuary, unaffected by gold mining activities.

These reference levels served to estimate I_{geo}, EF(Al) and EF(Fe) for all the studied elements in the Pra and Ankobra estuaries, which revealed moderate to significant enrichments in As, Ag and Cu.

In the Ankobra Estuary the probability of surpassing PEL was 77% for As, 50% for Cr and 27% for Ni; these values were of 13%, 23% and 10% for the Pra Estuary, and below 1% for the Volta.

Spatial maps of I_{geo} for As and Ag (related to their concentrations) suggested non-localized sources of contamination in the Pra and Ankobra estuaries. The lack of effect of particle sizes in the distribution of As concentrations in the Ankobra estuary suggests that they are associated to the transport and sedimentation of mining-tailing particles rather than to leaching processes from tailings dams.

Results from I_{geo} and EF reveal a moderate to significant impact of

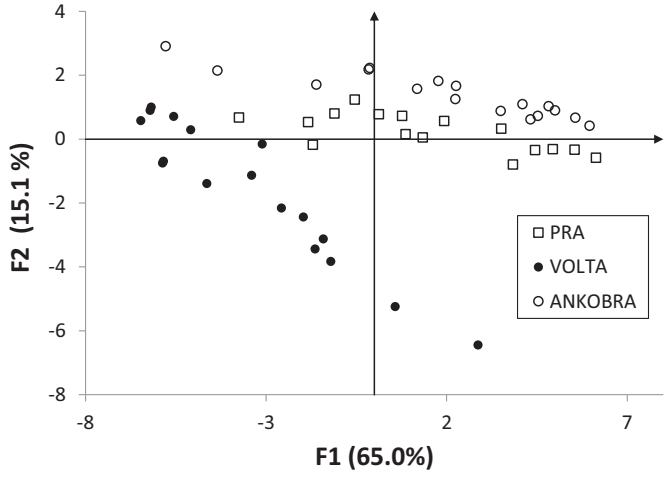

Fig. 9. Principal component analysis for the 50 studied sediment samples. Parentheses in labels report the percentage of variance explained by each component (see text). Samples from the three estuaries appear grouped into two distinct clusters.

gold-mining activity on As, Ag and Cu enrichment in two representative estuaries of West Africa and pose potential future implications on aquatic ecosystems and human health.

Acknowledgements

The authors would like to extend gratitude to the International Atomic Energy Agency (IAEA) for supporting the Regional Project RAF7009 and the fellowship GHA-16025, and to the Spanish Ministry of Economy and Competitiveness and the European Regional Development Fund of the European Union through the National Research, Development and Innovation Program for complementary funding (Plan Nacional I + d + i, Project AGl2014-57835-C2-1-R). Authors appreciate the technical support by Dr Oliva Polvillo from the Agricultural Research Service (SIA-CITIUS) of the University of Seville.

References

Abril, J.M., 1998. Basic microscopic theory of the distribution, transfer and uptake kinetics of dissolved radionuclides by suspended particulate matter - part I: theory development. J. Environ. Radioact. 41 (3), 307–324.

Abril, J., Fraga, E., 1996. Some physical and chemical features of the variability of K_d distribution coefficients for radionuclides. J. Environ. Radioact. 30 (3), 253–270.

Adjei-Kyereme, Y., Donkor, A.K., Golow, A.A., Yeboah, P.O., Pwamang, J., 2015. Mercury concentrations in water and sediments in rivers impacted by artisanal gold mining in the Asutifi District, Ghana. Res J. Chem. Environ. Sci. 3 (1), 40–48.

Allen, G.P., Salmon, J.C., Bassoullet, P., Penhoat, Y., De Grandpre, C., 1980. Effect of tides on mixing and suspended sediment transportation in macrotidal estuaries. Sediment. Geol. 26, 69–90.

Amonoo-Niezer, E.H., Nyamah, D., Bakiamoh, S.B., 1996. Mercury and arsenic pollution in soil and biological samples around the mining towns of Obuasi, Ghana. Water Air Soil Pollut. 91, 369–373.

Asante, K.A., Ntow, W.J., 2009. Status of environmental contamination in Ghana, the perspective of a research scientist. In: Obayashi, Y., Isobe, T., Subramanian, A., Suzuki, S., Tanabe, S. (Eds.), Interdisciplinary Studies on Environmental Chemistry — Environmental Research in Asia. TERRAPUB, pp. 253–260.

Bannerman, W., Potin-Gautier, M., Amouroux, D., Tellier, S., Rambaud, A., Babut, M., Adimado, A., Beinhoff, C., 2003. Mercury and arsenic in the gold mining regions of the Ankobra river basin in Ghana. J. Phys. IV 107, 107–110.

Barros, H., Laissaoui, A., Abril, J.M., 2004. Trends of radionuclide sorption by estuarine sediments. Experimental studies using ^{133}Ba as a tracer. Sci. Total Environ. 319, 253–267.

Bempah, C.K., Ewusi, A., Obiri-Yeboah, S., Asabere, S.A., Mensah, F., Boateng, J., Voigt, H.-J., 2013. Distribution of arsenic and heavy metals from mine tailings dams at Obuasi Municipality of Ghana. Int. J. Engine Res. 2 (5), 61–70.

Bryan, G.W., Langston, W.J., 1996. Bioavailability, accumulation and effects of heavy metals in sediments with special reference to United Kingdom estuaries: a review. Environ. Pollut. 76 (2) (89-13).

Chuhan-Pole, P., Dabalen, A.L., Land, B.C., 2017. Mining in Africa Are Local Communities Better Off? Agence Française de Développement and the World Bank (ISBN: 978-1-4648-0819-7).

Creed, J.T., Brockhoff, C.A., Martin, T.D., 1994. US-EPAMethod 200.8: determination of trace elements in waters and wastes by inductively coupled plasma-mass spectrometry. In: Environmental Monitoring Systems Laboratory Office of Research and Development, Revision 5.4EMMC Version. U.S. Environmental Protection Agency, Cincinnati, Ohio, USA.

Dimitrakakis, E., Hahladakis, J., Gidarakos, E., 2014. The "Sea Diamond" shipwreck: environmental impact assessment in the water column and sediments of the wreck area. Int. J. Environ. Sci. Technol. 11, 1421–1432.

Doe, K., Mroz, R., Tay, K.L., Burley, J., Tehc, S., Chend, S., 2017. Biological effects of gold mine tailings on the intertidal marine environment in Nova Scotia, Canada. Mar. Pollut. Bull. 114, 64–76.

Donkor, A.K., Bonzongo, J.C., Nartey, V.K., Adotey, D.K., 2005. Heavy metals in sediments of the gold mining impacted Pra River Basin, Ghana, West Africa. Soil Sediment Contam. 14, 479–503.

Donkor, A.K., Bonzongo, J.C., Nartey, V.K., Adotey, D.K., 2006. Mercury in different environmental compartments of the Pra River Basin, Ghana. Sci. Total Environ. 368, 164–176.

Enamorado-Báez, S.M., Abril, J.M., Gómez-Guzmán, J.M., 2013. Determination of 25 trace element concentrations in biological reference materials by ICP-MS following different microwave-assisted acid digestion methods based on scaling masses of digested samples. ISRN Anal. Chem. 1–14 (Article ID 851713).

Enamorado-Báez, S.M., Abril, J.M., Delgado, A., Más, J.L., Polvillo, O., 2014. Implications for food safety of the uptake by tomato of 25 trace-elements from a phosphogypsum amended soil from SW Spain. J. Hazard. Mater. 266, 122–131.

Enamorado-Báez, S.M., Gómez-Guzmán, Chamizo, E., Abril, J.M., 2015. Levels of 25 trace elements in high-volume air filter samples from Seville (2001 − 2002): sources, enrichment factors and temporal variations. Atmos. Res. 155, 118–129.

Ennouri, R., Zaaboub, N., Fertouna-Bellakhal, M., Chouba, L., Aleya, L., 2016. Assessing trace metal pollution through high spatial resolution of surface sediments along the Tunis Gulf coast (south-western Mediterranean). Environ. Sci. Pollut. Res. 23, 5322–5334.

Fashola, M.O., Ngole-Jeme, V.M., Babalola, O.O., 2016. Heavy metal pollution from gold mines: environmental effects and bacterial strategies for resistance. Int. J. Environ. Res. Public Health 13, 1047–1067.

Gelinas, Y., Barnes, R.M., Florian, D., Schmit, J.P., 1998. Acid leaching of metals from environmental particles: expressing results as a concentration within the leachable fraction. Environ. Sci. Technol. 32, 3622–3627.

Gerboles, M., Buzuca, D., Brown, R.J.C., Yardley, R.E., Hanus-Illnar, A., Salfinger, M., Vallant, B., Adriaenssens, E., Claeys, N., Roekens, E., Sega, K., Jurasovic, J., Rychlik, S., Rabinak, E., Tanet, G., Passarella, R., Pedroni, V., Karlsson, V., Alleman, L., Pfeffer, U., Gladtke, D., Olschewski, A., O'Leary, B., O'Dwyer, M., Pockeviciute, D., Biel-Cwikowska, J., Tursic, J., 2011. Interlaboratory comparison exercise for the determination of As, Cd, Ni and Pb in PM_{10} in Europe. Atmos. Environ. 45, 3488–3499.

Islam, M.S., Tanaka, M., 2004. Impacts of pollution on coastal and marine ecosystems including coastal and marine fisheries and approach for management: a review and synthesis. Mar. Pollut. Bull. 48, 624–649.

Klubi, E., Abril, J.M., Nyarko, E., Laissaoui, A., Benmansour, M., 2017. Radioecological assessment and radiometric dating of sediment cores from dynamic sedimentary systems of Pra and Volta estuaries (Ghana) along the equatorial Atlantic. J. Environ. Radioact. 178-179, 1–11.

Kumar, S.P., Edward, J.K.P., 2009. Assessment of metal concentration in the sediment cores of Manakudy estuary, south west coast of India. J. Mar. Sci. 38 (2), 235–248.

Lim, M., Han, G.C., Ahn, J.W., You, K.S., Kim, H.S., 2009. Leachability of arsenic and heavy metals from mine tailings of abandoned metal mines. Int. J. Environ. Res. Public Health 6, 2865–2879.

Link, D.D., Walter, P.J., Kingston, H.M., 1998. Development and validation of the new IPA microwave assisted beach method 3051A. Environ. Sci. Technol. 32, 3628–3632.

López-González, N., Borrego, J., Morales, J.A., Carro, B., Lozano-Soria, O., 2006. Metal fractionation in oxic sediments of an estuary affected by acid mine drainage (southwestern Spain). Estuar. Coast. Shelf Sci. 68, 297–304.

Loring, D.H., Rantala, R.T.T., 1992. Manual for the geochemical analyses of marine sediments and suspended particulate matter. Earth-Sci. Rev. 32, 235–283.

Macdonald, D.D., Carr, R.S., Calder, F.D., et al., 1996. Development and evaluation of sediment quality guidelines for Florida coastal waters. Ecotoxicology 5, 253–278.

Magesh, N.S., Chandrasekar, N.D., Vetha-Roy, D., 2011. Spatial analysis of trace element contamination in sediments of Tamiraparani estuary, southeast coast of India. Estuar. Coast. Shelf Sci. 92, 618–628.

Mahu, E., 2014. Geochemistry of estuarine sediments of Ghana: provenance, trace metal accumulation trends and ecotoxicological risks. In: Ph.D. Thesis. University of Ghana. http://ugspace.ug.edu.gh/handle/123456789/7278.

Meador, J.P., Ernest, D.W., Kagley, A., 2004. Bioaccumulation of arsenic in marine fish and invertebrates from Alaska and California. Arch. Environ. Contam. Toxicol. 47, 223–233.

Milési, J.P., Ledru, P., Ankrah, P., Johan, V., Marcoux, E., Vinchon, Ch., 1991. The metallogenic relationship between BMmian and Tarkwaian gold deposits in Ghana. Mineral. Deposita 26, 228–238.

Mil-Homens, M., Vale, C., Raimundo, J., Pereira, P., Brito, P., Caetano, M., 2014. Major factors influencing the elemental composition of surface estuarine sediments: the case of 15 estuaries in Portugal. Mar. Pollut. Bull. 84, 135–146.

Muller, G., 1969. Index of geo-accumulation in sediments of the Rhine River. Geochem. J. 2, 108–118.

NOAA, 2008. Screening Quick Reference Tables (SQuiRTs). https://repository.library.noaa.gov/view/noaa/9327.

Nude, P.M., Foli, G., Yidana, S.M., 2011. Geochemical assessment of impact of mine spoils on the quality of stream sediments within the Obuasi mines environment, Ghana. Int.

J. Geosci. 2, 259–266.

Oduro, W.O., Bayitse, R., Carboo, D., Kortatsi, B., Hodgson, I., 2012. Assessment of dissolved mercury in surface water along the lower basin of the river Pra in Ghana. J. Appl. Sci. Technol. 2 (1), 228–235.

Olmos, M.A., Birch, G.F., 2008. Application of sediment-bound heavy metals in studies of estuarine health: a case study of Brisbane Water estuary, New South Wales. Aust. J. Earth Sci. 55 (5), 641–654.

Pan, K., Wang, W.X., 2012. Trace metal contamination in estuarine and coastal environments in China. Sci. Total Environ. 3 (16), 421–422.

Pereira, T.S., Moreira, I.T.A., Oliveira, O.M.C., Rios, M.C., Filho, W.A.C.S., Almeida, N., Carvalho, G.C., 2015. Distribution and ecotoxicology of bioavailable metals and As in surfacesediments of Paraguaçu estuary, Todosos Santos Bay, Brazil. Mar. Pollut. Bull. 99, 166–177.

Petersson, A., Scherstén, A., Gerdes, A., 2018. Extensive reworking of Archaean crust within the Birimian terrane in Ghana as revealed by combined zircon U-Pb and Lu-Hf isotopes. Geosci. Front. 9, 173–189.

Pfeiffer, W.C., Lacerda, L.D., 1988. Mercury inputs into the Amazon Region, Brazil. Environ. Technol. Lett. 9, 325–330.

Postma, H., 1967. Sediment transport and sedimentation in the estuarine environment. In: Lauf, G.H. (Ed.), Estuaries. American Association for the Advancement of Science, Washington, DC, pp. 158–179.

Rajaee, M., Long, R.N., Renne, E.P., Basu, N.m, 2015. Mercury exposure assessment and spatial distribution in a Ghanaian small-scale gold mining community. Int. J. Environ. Res. Public Health 12, 10755–10782.

Rudnick, R.L., Gao, S., 2003. Composition of the continental crust. In: Turekian, K.K., Holland, H.D. (Eds.), Treatise on Geochemistry, 1st Edition. vol. 3. Elsevier Science, pp. 1–64 ISBN: 0-08-044338-9.

Sobrino-Figueroa, A.S., Becerra-Rueda, O.F., Magallanes-Ordóñez, V.R., Sánchez-González, A., Marmolejo-Rodríguez, A.J., 2015. Toxicity in semiarid sediments influenced by tailings of an abandoned gold mine. Environ. Monit. Assess. 187, 4158.

Suresh, G., Sutharsan, P., Ramasamy, V., Venkatachalapathy, R., 2012. Assessment of spatial distribution and potential ecological risk of the heavy metals in relation to granulometric contents of Veeranamlake sediments, India. Ecotoxicol. Environ. Saf. 84, 117–124.

Tarazona, J.V., Versonnen, B., Janssen, C., De Laender, F., Vangheluwe, M., Knight, D., 2014. Principles for Environmental Risk Assessment of the Sediment Compartment: Proceedings of the Topical Scientific Workshop. European Chemicals Agency, ECHA-14-R-13-EN.

Twining, J., Creighton, N., Hollins, S., Szymczak, R., 2008. Probabilistic risk assessment and risk mapping of sediment metals in Sydney Harbour embayments. Hum. Ecol. Risk. Assess. 14, 1202–1225.

US-EPA, 1995. SW-846 EPA method 3051 A. Microwave assisted acid digestion of sediments, sluges, soils and oils. In: Test Methods for Evaluating Solid Waste. 3rd Edition, 3rd Update. U.S. Environmental Protection Agency, Washington D. C..

US-EPA, 1996. Ecotox thresholds. In: Publication 9345.0-12FSI.EPA 540/F-95/038.PB95-963324.

Vesilind, P.A., 1980. The Rosin-Rammler particle size distribution. Resour. Recover. Conserv. 5 (3), 275–277.

Viers, J., Bernard Dupré, B., Gaillardet, J., 2009. Chemical composition of suspended sediments in World Rivers: new insights from a new database. Sci. Total Environ. 407, 853–868.

Wei, Ch., Wen, H., 2012. Geochemical baselines of heavy metals in the sediments of two large freshwater lakes in China: implications for contamination character and history. Environ. Geochem. Health 34 (6), 737–748.

World Bank, 2012. Increasing local procurement by the mining industry in West Africa. In: Report No. 66585-AFR.

Xu, Y., Sunb, Q., Yi, L., Yin, X., Wang, A., Li, Y., Chen, J., 2014. The source of natural and anthropogenic heavy metals in the sediments of the Minjiang River Estuary (SE China): implications for historical pollution. Sci. Total Environ. 493, 729–736.

Zitko, V., 1994. Principal component analysis in the evaluation of environmental data. Mar. Pollut. Bull. 28 (12), 718–722.